Development of a Personalized Intestinal Fibrosis Model Using Human Intestinal Organoids Derived From Induced Pluripotent Stem Cells

Hannah Q. Estrada, BS,[*,#] **Shachi Patel, MS,**[*,#] **Shervin Rabizadeh, MD,**[†] **David Casero, PhD,**[‡]
Stephan R. Targan, MD,[‡] **and Robert J. Barrett, PhD**[*,‡]

From the *Board of Governors Regenerative Medicine Institute, Cedars-Sinai Medical Center, Los Angeles, CA, USA;
[†]Division of Pediatric Gastroenterology, Cedars-Sinai Medical Center, Los Angeles, CA, USA; and
[‡]F. Widjaja Foundation Inflammatory Bowel and Immunobiology Research Institute, Cedars-Sinai Medical Center, Los Angeles, CA, USA.
[#]H.Q.E. and S.P. contributed equally.

Address correspondence to: Robert J. Barrett, PhD, Board of Governors Regenerative Medicine Institute and F. Widjaja, Foundation Inflammatory Bowel and Immunobiology Research Institute, Cedars-Sinai Medical, Center, Advanced Health Sciences Pavilion 8308, 8700 Beverly Blvd, Los Angeles, CA 90048, USA (robert.barrett@cshs.org).

Background: Intestinal fibrosis is a serious complication of Crohn's disease. Numerous cell types including intestinal epithelial and mesenchymal cells are implicated in this process, yet studies are hampered by the lack of personalized in vitro models. Human intestinal organoids (HIOs) derived from induced pluripotent stem cells (iPSCs) contain these cell types, and our goal was to determine the feasibility of utilizing these to develop a personalized intestinal fibrosis model.

Methods: iPSCs from 2 control individuals and 2 very early onset inflammatory bowel disease patients with stricturing complications were obtained and directed to form HIOs. Purified populations of epithelial and mesenchymal cells were derived from HIOs, and both types were treated with the profibrogenic cytokine transforming growth factor β (TGFβ). Quantitative polymerase chain reaction and RNA sequencing analysis were used to assay their responses.
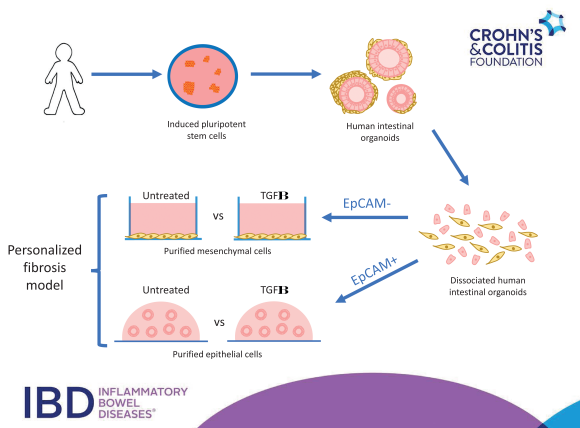
Results: In iPSC-derived mesenchymal cells, there was a significant increase in the expression of profibrotic genes (Col1a1, Col5a1, and TIMP1) in response to TGFβ. RNA sequencing analysis identified further profibrotic genes and demonstrated differential responses to this cytokine in each of the 4 lines. Increases in profibrotic gene expression (Col1a1, FN, TIMP1) along with genes associated with epithelial-mesenchymal transition (vimentin and N-cadherin) were observed in TGFβ -treated epithelial cells.

Conclusions: We demonstrate the feasibility of utilizing iPSC-HIO technology to model intestinal fibrotic responses in vitro. This now permits the generation of near unlimited quantities of patient-specific cells that could be used to reveal cell- and environmental-specific mechanisms underpinning intestinal fibrosis.

Lay Summary

Intestinal fibrosis is a serious complication of Crohn's disease and novel in vitro models are urgently needed to study this. We describe an induced pluripotent stem cell–derived modeling system whereby a near unlimited number of both epithelial and mesenchymal cells could be used in a personalized intestinal fibrosis model.

Graphical Abstract

Introduction

Intestinal fibrosis is a serious complication of Crohn's disease (CD) with 20%-30% of patients requiring surgery within 20 years of diagnosis,[1,2] and this incidence remains stubbornly high despite significant improvements in controlling inflammation.[3-5] Currently, there are no therapies to prevent the onset of intestinal fibrosis, and this was underscored in the RISK study whereby early anti-tumor necrosis factor α intervention failed to prevent the onset of this complication.[6] New human cellular models that would permit either mechanistic studies or the development of antifibrotic

therapies are urgently needed but are hampered by the relative difficulty in procuring cells from this patient population. Such procurement requires invasive procedures such as endoscopy or surgical resection and is limited to those who require them. In addition, given the profound genetic heterogeneity in CD patients,[7] coupled with the profound heterogeneity in the intestinal fibrotic phenotype,[8] the procurement process may be even more challenging if potential studies require cells from specific CD patients based on genotype or phenotype. Therefore, it is highly desired to develop a personalized intestinal fibrosis model, which incorporates
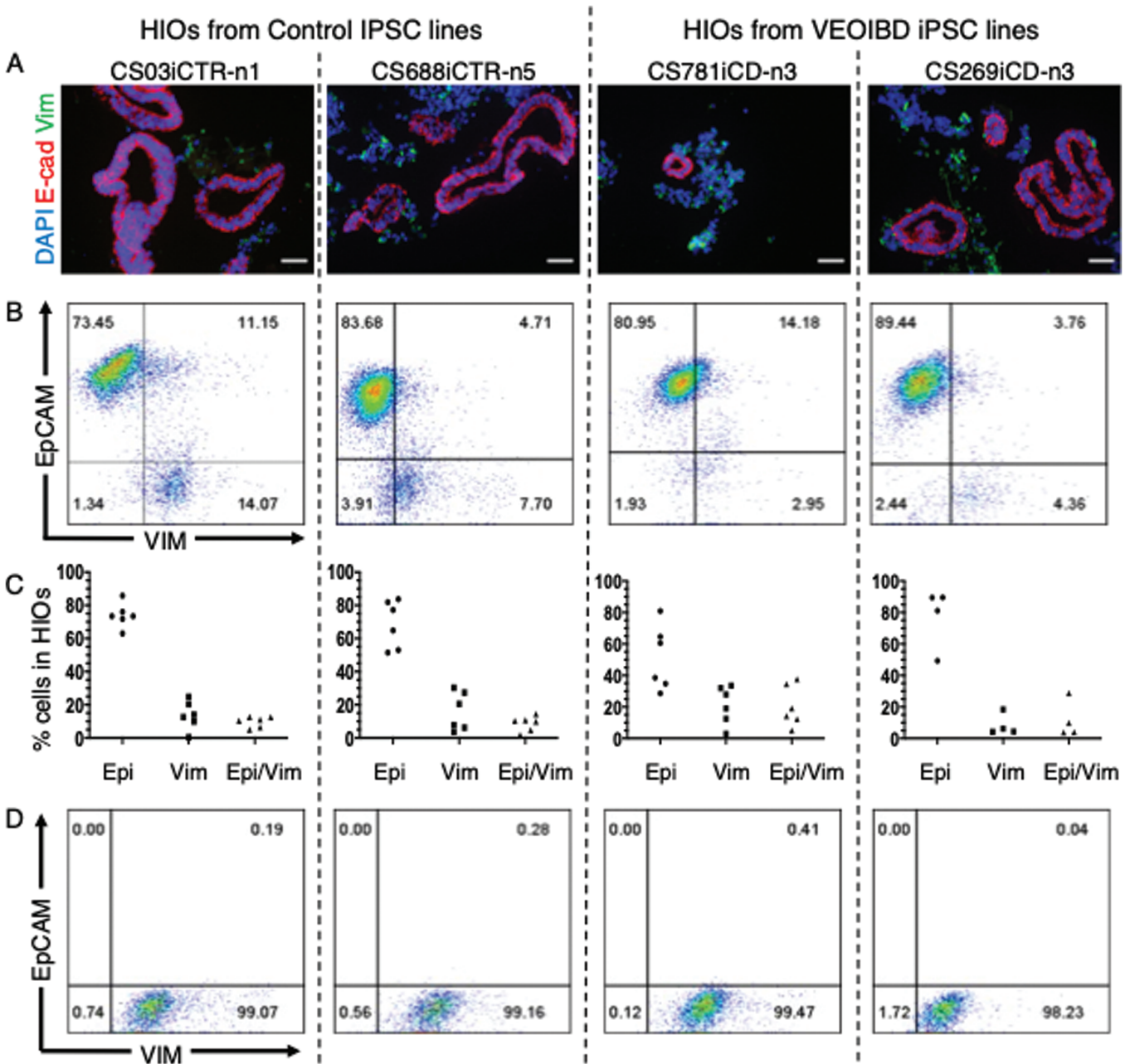

FIGURE 1. Characterization of induced pluripotent stem cell (iPSC)–derived human intestinal organoids (HIOs) and purified mesenchymal cell population. A, Representative images showing iPSC-derived HIOs immunopositive for E-cadherin (E-cad) (red) and vimentin (Vim) (green), and all counterstained with DAPI (blue). Scale bar = 50 μm. B, Representative dot plot showing populations of EpCAM+ and vimentin+ cells in HIOs derived from each iPSC line. C, Graph showing cellular populations in HIOs from 4-6 directed differentiations of each individual's iPSC line. D, Representative dot plot of purified populations of iPSC-derived mesenchymal cells. VEOIBD, very early onset inflammatory bowel disease.
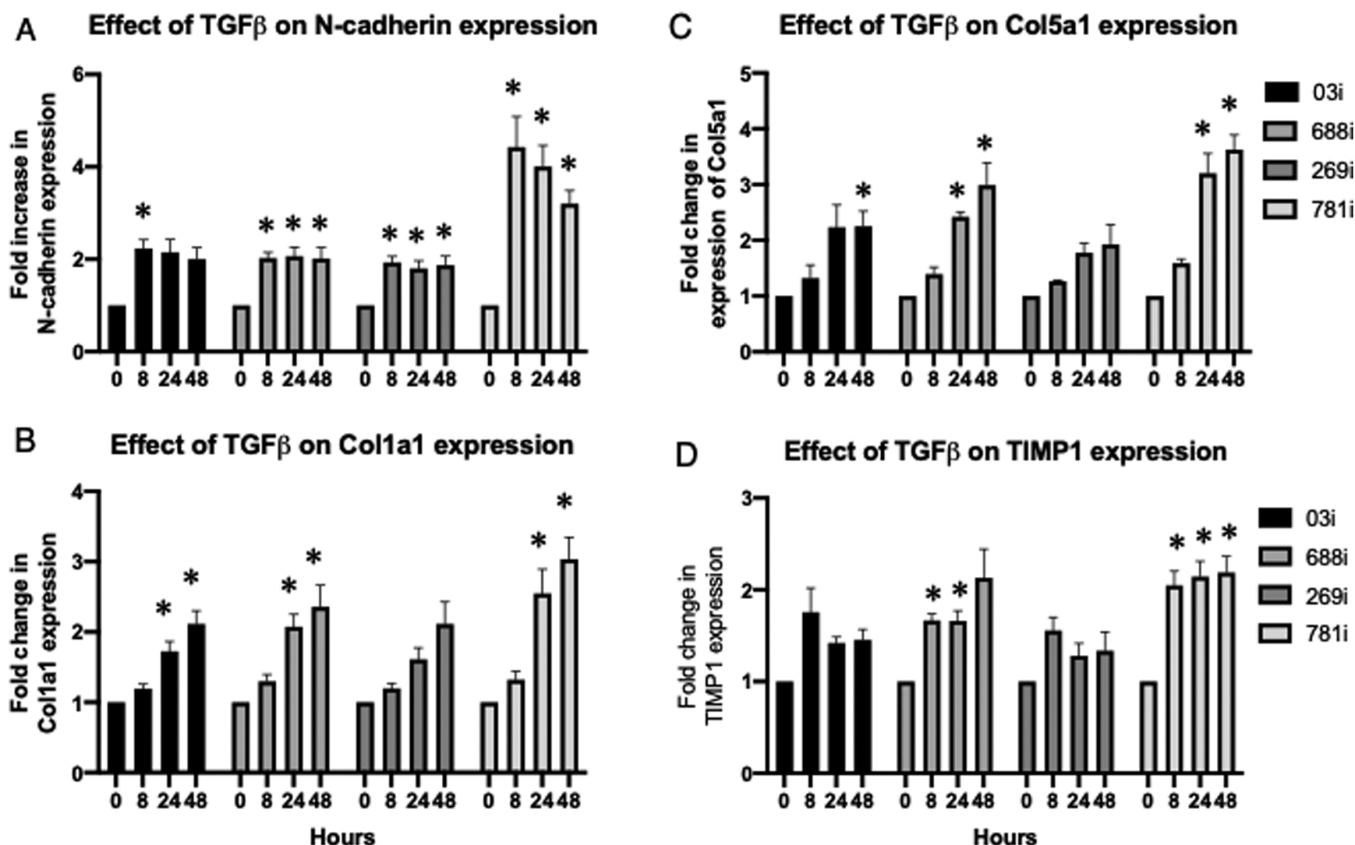
FIGURE 2. Characterization of fibrotic response in transforming growth factor β (TGFβ)–treated induced pluripotent stem cell–derived mesenchymal cells over time. Fold-change increases in (A) N-cadherin, (B) Col1a1, (C) Col5a1, and (D) TIMP1 were assessed after 8, 24, and 48 hours of TGFβ (1 ng/mL) treatment. Data were obtained from 16 independent experiments whereupon mesenchymal cells were obtained from 4 passages of induced pluripotent stem cell–derived organoids, and each passage was examined 4 times. Data obtained from a 2-way analysis of variance with a post hoc Dunnett's test was carried out to determine for statistical significance in the 8-, 24-, and 48-hour time points as compared with each respective control (time 0) time point. $*P < .05$.

biologically relevant cell types, that could be generated from a cellular source by relatively noninvasive means.

Human intestinal organoids (HIOs) derived from induced pluripotent stem cells (iPSCs) represents one avenue that is particularly amenable to the development of such a model. First, iPSCs can be generated from almost any individual and a range of donor cell types, including peripheral blood mononuclear cells, which are easily obtained from a simple blood draw, can be reprogrammed to generate this cell type.[9] Second, iPSCs retain the genetics of the reprogrammed donor cells, meaning that personalized responses in iPSC-derived cell types can be assayed. Third, while biopsy-derived intestinal organoids possess only an epithelial cell population,[10,11] iPSC-derived HIOs also contain a mesenchymal cell population[12-14] meaning that both epithelial and mesenchymal cells, both of which are implicated in intestinal fibrosis,[15-18] can be studied using this system. Finally, the feasibility of using the organoid approach has previously been demonstrated when it was shown that the effects of various antifibrotic therapeutics could be assayed using HIOs derived from embryonic stem cells.[19,20] However, to date, no studies have demonstrated that iPSC-derived HIOs, generated from actual patients, could be used to assay fibrotic responses.

In this study, we aimed to demonstrate the feasibility of utilizing iPSC-derived HIOs to generate a personalized model of intestinal fibrosis. To this end, we obtained iPSCs from 2 unaffected control subjects and from 2 very early onset inflammatory bowel disease (VEOIBD) patients who had stricturing complications and directed all 4 iPSC lines to form HIOs. Given that the ratio of epithelial and mesenchymal cells is variable in HIO culture, we obtained purified populations of both cell types and assayed their response to transforming growth factor β (TGFβ), a cytokine well known to be implicated in intestinal fibrosis.[21] Here, we demonstrate that iPSC-derived mesenchymal cells, in response to TGFβ, consistently upregulate the expression of a number of fibrosis-related genes, while line-specific sensitivity to TGFβ stimulation could also be detected for a number of these genes. Additionally, the effects of the TGFβ on iPSC-derived intestinal cells both in terms of measuring epithelial-mesenchymal transition (EMT) changes and the fibrotic response could also be assayed.

Methods

Ethics Statement

All the cell lines and protocols in the present study were carried out in accordance with the guidelines approved by the stem cell research oversight committee and institutional review board at the Cedars-Sinai Medical Center under the auspice of the institutional review board stem cell research oversight committee protocols Pro00055055 (a personalized intestinal fibrosis model combining patient specific iPSC-derived human intestinal organoids and small microengineered chip

technology). All authors had access to the study data and have reviewed and approved the final manuscript.

Cell Lines and Culturing Conditions

Two iPSC lines (CS03iCTR-n1 and CS688iCTR-n5) were obtained from the iPSC Core at Cedars-Sinai Medical Center and were both derived from healthy control subjects. The CS269iCD-n3 iPSC line was derived from a VEOIBD patient who was diagnosed at the age of 2 years and has a history of severe fibrostenosing CD that has resulted in multiple small bowel resections for stricturing CD. The CS781iCD-n3 iPSC line was generated from a VEOIBD patient who was diagnosed at the age of 4 years, and who has recurrent endoscopic dilatation owing to observed stricturing. All lines were fully characterized for pluripotency markers and were confirmed to be karyotypically normal. They were maintained in an undifferentiated state on Matrigel-coated plates in mTeSR1 media (Stem Cell Technologies, Vancouver, BC, Canada) under feeder-free conditions.

Generation of HIOs From iPSCs

The generation of HIOs from iPSCs involves a multistep technique whereby iPSCs were directed to form definitive endoderm, hindgut structures and ultimately organoids and has been previously described.[13,14] All HIOs were cultured in media containing CHIR99021 (2 μM; Tocris, Ellisville, MO, USA), noggin and EGF (both 100 ng/mL; all R&D Systems, Minneapolis, MN, USA), and B27 (1×; Invitrogen, Waltham, MA, USA) in Advanced Dulbecco's modified Eagle medium F/12 with penicillin/streptomycin and L-glutamine (5% v/v). Organoids were passaged after 7-10 days and ultimately either processed for immunocytochemistry or flow cytometry or magnetic-activated cell sorting (MACS) after 12-18 days.

Immunohistochemistry and Microscopy

HIOs were fixed in 4% paraformaldehyde (Electron Microscopy Sciences, Hatfield, PA, USA), transferred to 30% sucrose overnight at 4 °C, embedded in Tissue-Tek O.C.T Compound (VWR, Radnor, PA, USA), and cut into 10-μm sections. Sections were blocked in 10% normal donkey serum (Jackson ImmunoResearch, West Grove, PA, USA) with 0.5% Triton X-100 and incubated with the following primary antibodies: goat anti-mouse/human E-cadherin (AF648; R&D Systems) and mouse anti-vimentin (#550513; BD Biosciences, San Jose, CA, USA) for either 4 hours at room temperature or overnight at 4 °C. Sections were then rinsed and incubated in species-specific AF488 or AF647-conjugated secondary antibodies (Life Technologies, Carlsbad, CA, USA) followed by DAPI (0.5 μg/mL; Life Technologies, Carlsbad, CA, USA) to counterstain nuclei and were imaged using a Leica DM6000 B microscope (Leica, Wetzlar, Germany).

Flow Cytometry

HIOs were removed from Matrigel and washed 3-4 times in phosphate-buffered saline and subsequently incubated in TrypLE Express (Life Technologies, Camarillo, CA, USA) for 2-3 minutes until the organoids were completely dissociated to a single cell suspension. Single cells were then fixed and permeabilized using Flow Cytometry Fixation & Permeabilization Buffer Kit I (R&D Systems). Cells were then stained with the following fluorophore-conjugated antibodies: mouse anti-human EpCAM (# 324212; BioLegend, San Diego, CA, USA) and mouse anti-human vimentin (#562338; BD Pharmingen, San Diego, CA, USA). Cells were analyzed on a BD Fortessa Cell Analyzer (BD Biosciences) and flow cytometry analysis was carried out using FlowJo software (FlowJo, Ashland, OR, USA).

Generation of Purified Epithelial and Mesenchymal Cell Cultures

HIOs were dissociated to a single cell suspension as described previously. Dissociated cells were incubated with CD326/EpCAM MicroBeads (Miltenyl Biotec, San Diego, CA, USA) for 30 minutes at 4 °C, and EpCAM+ and EpCAM– populations of cells were obtained via MACS. EpCAM+ cells were cultured as epithelial-only HIOs (eHIOs) as previously described.[13] Briefly, EpCAM+ cells were maintained in organoid media supplemented with SB202190 (10 μM; Tocris) and A83-01 (500 nM; Tocris). EPCAM– cells were cultured in advanced Dulbecco's modified Eagle medium media containing 10% fetal calf serum and were passaged weekly.

In Vitro TGFβ Fibrosis Model

eHIOs were cultured in HIO media (depleted of SB202190 and A83-01) for 24 hours and were treated with either 0.5 or 1 ng/mL of TGFβ (R&D Systems) for 48 hours. For determining TGFβ responses in mesenchymal cells, 1×10^5 cells were seeded in 24 well plate plates for 72 hours, then depleted of serum for 24 hours and subsequently treated with 1 ng/mL of TGFβ for described time points.

Quantitative Real-Time Polymerase Chain Reaction

Both epithelial and mesenchymal cells were extracted in situ with the RNeasy mini kit (Qiagen, Germantown, MD, USA). Complementary DNA was generated from 1 μg of RNA using the Omniscript RT Kit (Qiagen). Quantitative real-time polymerase chain reaction was performed using SYBR Select Master Mix (Applied Biosystems, Carlsbad, CA, USA) on a BioRad CFX384 Real-Time System (Bio-Rad, Hercules, CA, USA). Primer sequences are listed in Supplementary Table 1.

RNA Sequencing Data Analysis

The STAR ultrafast universal RNA sequencing aligner v2.7.3a[22] was used to generate the genome index and perform single-end alignments. Reads were aligned to a genome index that includes both the genome sequence (GRCh38 primary assembly) and the exon-intron structure of known gene models (Gencode genome annotation version 33). Alignment files were used to generate gene-level count summaries with STAR's built-in gene counter. Only protein-coding genes in the Gencode 33 annotation were considered (>98% of total counts for all samples). Independent filtering was applied as before[23]: genes with <1 average count per sample, count outliers, or low mappability were filtered out for downstream analysis. Counts were normalized persample in units of transcripts per million after correcting for gene mappable length and per-sample sequencing depth. However, count-based normalized and variance-stabilized data (see the following) was used for all ordination, differential, clustering, and variance analyses, and all figures unless otherwise noted.

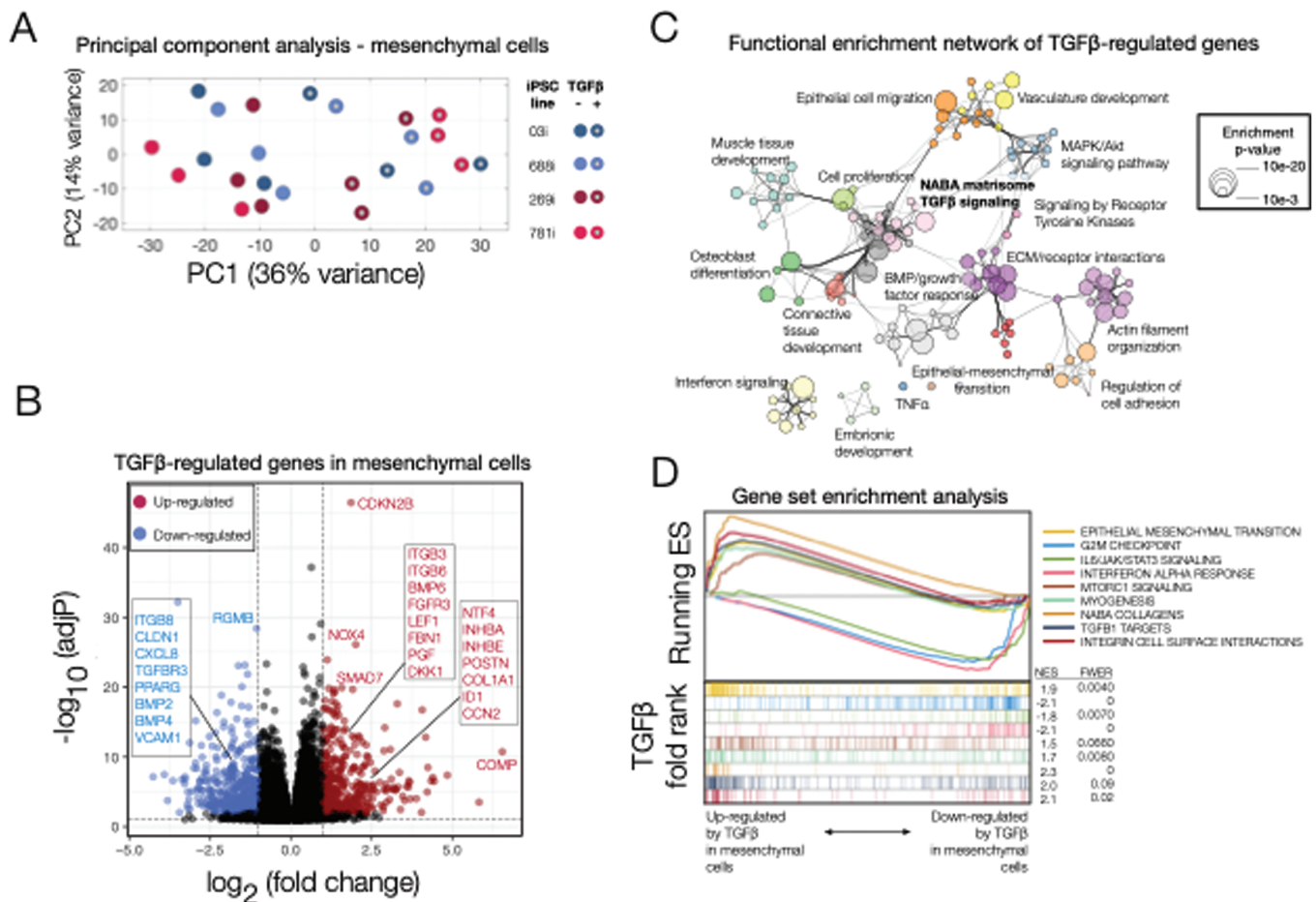Principal component analysis of TGFβ-treated mesenchymal cells (Figure 3A) was performed using as input the

FIGURE 3. Transcriptional responses to transforming growth factor β (TGFβ) in induced pluripotent stem cell (iPSC)–derived mesenchymal cells. A, Principal component analysis (PCA) of gene expression for TGFβ-treated and untreated mesenchymal cells purified from iPSC-derived human intestinal organoids. The first 2 components (principal component 1 [PC1], PC2) are shown along with the percent of gene expression variance explained. Clustering was obtained using variance-stabilized data after correction for batch- and line-specific baseline expression, and from all expressed human genes without additional filters. Data are representative of 3 independent replicates for each experimental group (24 samples total). B, Volcano plot summarizing the global effect of TGFβ treatment on gene expression levels. Fold changes and adjusted *P* values correspond to a log-likelihood ratio test (LRT) on treated vs untreated cells independent of source (iPSC line). Highlighted are selected upregulated (red) and downregulated (blue) genes (more than a 2-fold change after TGFβ treatment, LRT-adjusted *P* < .01). C, Functional enrichment network for all genes differentially regulated by TGFβ (more than a 2-fold change after TGFβ treatment, LRT adjusted *P* < .01). Individual Gene Ontology terms with similar gene members are grouped by categories (node color) and labeled using a representative member. Node size is proportional to statistical significance (enrichment *P* value) as shown. Edge thickness is proportional to between-node similarity and reflects the overlap between genes annotated in both ontology terms. Only edges representing a kappa similarity score >0.3 are shown. Only significant ontology terms are shown (hypergeometric-adjusted *P* value < 1 × 10^{-3}). Members of selected ontologies are presented in Table 1. D, Gene set enrichment analyses of selected enriched pathways in TGFβ-treated mesenchymal cells. The x-axis represents the preranked list of genes based on the fold change between treated and untreated cells as in B, with genes highly upregulated by TGFβ in our human intestinal organoids positioned to the left. Segment plots (bottom) highlight the position of genes from independent reference pathways (eg, epithelial-mesenchymal transition) in ranked list. The vertical axis in line plots (top) represents the cumulative enrichment score (ES) from gene set enrichment analysis, and normalized ES is the overall normalized enrichment score (with familywise error rate) for each selected pathway. TNFα, tumor necrosis factor α.

residuals from a model that corrected for batch- and line-specific baseline expression levels.[24] Differential expression analysis was performed with DESeq2.[25] Count data were fitted using generalized linear models using batch and iPSC line as explanatory factors to correct for batch- and line-specific baseline expression levels, and testing for a global additive effect of treatment (Figure 3B) or an interaction between treatment and iPSC line (Figure 4C). A gene was classified as differentially expressed using appropriate thresholds for adjusted *P* value (likelihood ratio test) and log2 fold-change if applicable. Line-specific genes (Figure 4B) were identified using a model correcting Batch and testing for iPSC line with 2 levels to test for differences between gene expression in one line as compared with all others. Genes were classified as line type–specific if the Wald adjusted *P* value was <.05.

Functional enrichment was performed with Metascape[26] and enrichment statistics presented as hypergeometric adjusted *P* values. The networks of ontology terms (Figure 3C) were computed in house and visualized with Cytoscape.[27] Nodes with the same color are specific ontologies in the same Gene Ontology generic class and were labeled using a representative member or generic name. Node size is proportional to statistical significance (hypergeometric *P* value). Edge thickness is proportional to between-node similarity and was computed in house in MATLAB (version release 2020ba; The MathWorks, Inc, Natick, MA, USA; RRID:SCR_001622)

using kappa statistics[28] and reflects the overlap between the gene sets annotated in both ontology terms. Fold changes from the various generalized linear models above (Figure 3C) were employed to perform gene set enrichment analysis[29] using gene expression signatures from independent studies.. The global, line-independent response to TGFβ (Figure 3C) was analyzed by ranking genes based on their TGFβ-induced fold changes and estimating the enrichment of gene signatures from the Molecular Signatures Database (MSigDB).[30,31] The same was applied to genes ranked by their response to TGFβ in each iPSC line independently (Figure 4A). All plots were generated in R (R Foundation for Statistical Computing, Vienna, Austria) and MATLAB.

Statistical Analysis

All data are represented as mean ± SEM. Statistical analysis was carried out using GraphPad Prism 9 software (GraphPad Software, San Diego, CA, USA) using a 1-way analysis of variance with a post hoc Dunnett's test or a Kruskal-Wallis test. Differences between groups were considered statistically significant when $P < .05$.

Results

iPSC-Derived HIOs Contain Varying Numbers of Mesenchymal and Epithelial Cells

iPSCs were generated from 2 control individuals (CS03iCTR-n1, CS688iCTR-n5) and 2 VEOIBD patients with stricturing complications (CS269iCD-n3, CS781iCD-n3), and all 4 iPSC lines were directed to generate HIOs. In contrast to biopsy-derived intestinal organoids, iPSC-derived HIOs have previously been reported to contain both epithelial and mesenchymal cells,[13,14] and we similarly report via immunocytochemistry that HIOs from all 4 iPSC lines contain both an epithelial (E-cadherin+) and a mesenchymal cell (vimentin+) population (Figure 1A). To determine how variable these populations were, iPSCs from all 4 individuals were serially passaged 4-6 times, and each passage was directed to form HIOs. These were subsequently assessed after 12-18 days by dissociating HIOs to a single cell suspension and quantifying the epithelial (EpCAM+) and mesenchymal (vimentin+) population via flow cytometry (Figure 1B). We found that HIOs from 3 of the 4 lines generated organoids that were composed primarily of epithelial cells, but there was considerable variability in both the epithelial-only (EpCAM+/vimentin–) and mesenchymal-only (EpCAM–/vimentin+) cell populations, even in HIOs derived from the same iPSC line (Figure 1C).

Given this variability, we determined to assay fibrotic responses only in purified populations of both cell types. We have previously demonstrated that purified populations of epithelial cells could be obtained from HIO cultures by dissociating them to a single cell suspension, and positively selecting for EpCAM via MACS.[13,14] In order to obtain purified cultures of mesenchymal cells, we adapted this protocol and plated the EpCAM– population in Advanced Dulbecco's modified Eagle medium media containing 10% fetal calf serum. These cells could be serially passaged up to 10-15 times, and flow cytometry analysis revealed they were primarily composed (> 98%) of mesenchymal (vimentin+) cells with virtually no epithelial (EpCAM+) cells (Figure 1D). The derivation of purified populations of epithelial and mesenchymal cells from control- and patient-specific HIOs thus

provides a platform to assay fibrotic responses in both cell types under a tightly control milieu.

Fibrotic Responses Can Be Assayed in TGFβ-Treated iPSC-Derived Mesenchymal Cells

Having established the culturing conditions to generate purified iPSC-derived mesenchymal cells, we then wished to examine if these could be used to assay responses to TGFβ, a cytokine well known to be implicated in intestinal fibrosis.[21] iPSC-derived mesenchymal cells from all 4 lines were cultured with 1 ng/mL of TGFβ and assayed after 8, 24, and 48 hours. We initially examined N-cadherin, as this has previously been shown to be upregulated in TGFβ-treated intestinal fibroblasts,[32] and we report a significant fold increase in expression after 8 hours, which was mostly maintained up the 48 hour time point (Figure 2A). We examined for changes in Col1a1 expression and found it was significantly increased in 3 of the 4 lines after 24 hours and ultimately reached a maximal expression at 48 hours (Figure 2B). While secretion of collagen could be assayed via a Sircol assay, we did not observe any significant change in secretion from any of the 4 lines (data not shown). Col5a1 was previously found increased in the RISK cohort with stricturing complications, and we similarly report a significant increase in the 781i line (Figure 2C). We also examined for TIMP1, shown to be upregulated in myofibroblasts obtained from resected fibrotic tissue of CD patients,[33,34] and report an increase after in all 3 timepoints in the 781i line (Figure 2D). Thus, we demonstrate that biologically relevant fibrotic responses can be assayed in TGFβ-treated iPSC-derived mesenchymal cells.

Transcriptional Responses to TGFβ in iPSC-Derived Mesenchymal Cells

Having observed that a robust TGFβ-mediated fibrotic response was observed at the 48-hour time point, we performed whole-transcriptome analyses (RNA-Seq) on treated and untreated iPSC-derived mesenchymal cells derived the same 4 iPSC-derived HIOs. First, we aimed to test the hypothesis that our system can be used to model known, generic responses to TGFβ in all cell lines. To this end, we regressed out the effect of both technical (eg, batch) and line-specific factors on baseline expression levels using multivariate linear modeling (see Methods for details). Principal component analysis of the corrected expression levels revealed a complete segregation between treated and untreated samples, suggesting a robust and reproducible contribution of TGFβ to gene expression trends common to all 4 iPSC lines (Figure 3A). Differential analysis identified a set of 570 genes significantly and strongly regulated by TGFβ (likelihood ratio test [LRT] adjusted P value <.01, log2 fold-change >1) even after correcting for technical and line-specific expression variability (Figure 3B). Functional enrichment analysis on this set of significantly regulated genes revealed a highly connected functional network recapitulating both mesenchyme- and TGFβ-related terms (Figure 3C), including a backbone of pathways consisting of TGFβ-signaling, NABA matrisome and several other related with extracellular matrix structure and signaling. Enrichment and gene membership results for selected ontologies are shown in Table 1, which further highlights that the common response observed in all our iPSC lines

TABLE 1. Selected Ontologies Significantly Associated With the Response to TGFβ Treatment in Mesenchymal Cells Derived From Human Intestinal Organoids

Pathway	q Value	Regulated/Total	Upregulated by TGFβ	Downregulated by TGFβ
Epithelial-mesenchymal transition	1×10^{-68}	92/200	ACTA2, ADAM12, ADAM19, ADAMTS10, ADAMTS16, ADAMTS2, ADAMTS4, ADAMTS6, AEBP1, ANOS1, APLP1, B4GALT1, BGN, CALD1, CCN2, CDH11, CDH2, CILP2, CILP, CILP2, COL10A, COL11A1, COL12A1, COL16A1, COL1A1, COL24A, COL25A1, COL3A1, COL4A1, COL4A2, COL5A1, COL5A2, COL6A3, COL7A1, COL8A1, COL8A2, COL9A2, COMP, CREB3L1, CRISPLD2, CRLF1, DKK1, DPT, ELN, EMILIN1, MFAP4, MFAP2, FAP, CFAP44, MFAP3L, FBLN5, FBN1, FERMT2, FN1, FNDC1, FSTL3, FZD8, GADD45B, GPX7, GREM1, HAPLN3, HMCN1, IGFBP3, IGFBP7, INHBA, ITGA1, ITGA11, ITGA8, ITGAV, ITGB1BP2, ITGB1, ITGB3, ITGB5, ITGB6, JUNB, KAZALD1, LAMC2, LOX, ALOX5AP, LOXL3, LOXL3, LRP12, LRP1, LRRC15, LTBP1, LTBP2, MATN3, MFAP2, MFAP4, MMP16, MMP2, MXRA5, MYL9, P3H1, P3H4, P4HA1, P4HA2, P4HA3, PDGFA, PHLDB1, PLOD1, PMEPA1, PODNL1, PODNL1, POSTN, PRG4, RUNX1, PSAT1, SCX, SDC1, SERPINE2, SERPINH1, SGCD, SGCG, SH3PXD2A, SPARC, SRPX2, TAGLN, TGFB1, TGFB3, TGFBI, TGM2, THBS1, TIMP3, TNC, TNFAIP6, TPM1, TPM2, VCAN	ANPEP, BMPER, COL21A1, COL4A6, CRISPLD1, CXCL1, CXCL16, CXCL6, CXCL8, DAB2, DCN, EFEMP1, AFAP1L2, TFAP4, GAS1, IGFBP6, IGSF10, IL15, IL32, ITGA10, JUN, LAMA4, MATN2, MCM7, MEST, NTN1, NTN4, NTNG1, OXTR, PAPLN, PODN, PRELP, PTX3, RGS4, SAT1, SDC4, SFRP1, SLIT2, SNTB, SRGN, SVEP1, TGFBR3, THSD4, VCAM1, VWA5A, VWCE
ECM organization	1×10^{-45}	71/395		
ECM glycoproteins	1×10^{-20}	48/196		
Interferon signaling	1×10^{-28}	46/200	IFITM10	ANPEP, APOBEC3B, APOBEC3F, APOBEC3G, BST2, C1RL, C1R, CAMK2D, CASP4, CAV1, CCL2, CDK18, CDK1, CFH, CLDN11, CLDN1, CSF1, CXCL6, CXCL8, DCLK1, DDX58, DDX60, DHX58, DPP4, DTX3L, EGFR, F2RL1, FAM111A, FOSL1, HELZ2, HERC6, HMGA1, HMGA2, ICAM1, IFI16, IFI35, IFI44, IFI6, IFIH1, IFIT1, IFIT2, IFIT3, IFIT5, IFITM1, IFITM2, IFITM3, IL15, IRF1, IRF2, ITGB8, LGALS3BR, MID1, MX1, NEDD4L, NFIA, NMI, NRP1, OAS3, PARP10, PARP12, PARP14, PARP9, PLSCR1, POLR3G, PSMB8, PSMB9, PSME1, PTX3, SAMHD1, SECTM1, SLC20A2, SOCS1, SOCS3, SOD2, SP110, STING1, STMN1, STOM, TNFAIP2, TNFSF10, TRIM14, TRIM25, TXNIP, UBE2L6, USP18, VCAM1, VWCE
Cell cycle	1×10^{-30}	45/200		ASF1B, ATAD2, AURKA, BRCA1, BUB1B, CDC25B, CDC25A, CDC45, CDCA3, CDCA8, CDK18, CDK1, CENPM, CHAF1A, CITED2, CIT, CKS1B, CKS2, E2F1, EFNA5, EXO1, GINS1, GINS2, GINS3, GINS4, HELLS, HMGA1, HMGB2, KIF11, KIF15, KIF20B, KIF22, LMNB1, MAD2L1, MCM2, MCM3, MCM4, MCM5, MCM7, MELK, MXD3, NEK2, ORG6, PBK, PRIM2, RACGAP1, RAD51AP1, RAD54L, RBL1, RFC3, RNASEH2A, RRM2, SAP30, SHMT1, SMAD3, SPC24, STMN1, TACC3, TCF19, TIMELESS, TK1, TPX2, TRAIP, TRIP13
Response to TGFβ	1×10^{-17}	50/261	CDKN2B, CHST11, CILP2, CILP, COL1A1, COL3A1, COL4A2, DKK3, EMILIN1, FBN1, FERMT2, ID1, ITGB1BP2, ITGB1, ITGB5, ITGB6, JUNB, LOX, ALOX5AP, LOXL3, LRRC32, LTBP1, LTBP2, MXRA5, MYOCD, NOX4, PMEPA1, POSTN, RASL11B, SCX, SKIL, SMAD7, SNX25, TGFB1, TGFB3, THBS1	CAV1, CITED2, CLDN1, CLDN11, CLEC3B, DAB2, GDF5, HTRA3, MID1, ITGB8, JUN, PDE3A, PDGFD, PEG10, SFRP1, SMAD1, SMAD3, SPRY1, TGFBR2, TGFBR3, ZFP36L2

Specific terms were selected from the summary enrichment shown in Figure 3. Shown are the individual hypergeometric q values for each ontology, the number of genes significantly regulated by TGFβ regardless of source (induced pluripotent stem cell line) along with the total number of human genes annotated in each ontology (regulated/total), and official gene symbols for both up and downregulated genes after treatment with TGFβ.

Abbreviations: ECM, extracellular matrix; TGFβ, transforming growth factor β.

comprises numerous genes previously associated with TGFβ signaling and intestinal fibrosis. We further evaluated the directionality and extent of the observed functional shifts. Using gene set enrichment analysis, we summarized changes in expression for entire pathways or ontologies after TGFβ treatment (Figure 3D). This supervised analysis revealed a significant (familywise error rate < 0.1, normalized enrichment score > 1.9) global upregulation of several functional groups including EMT, NABA collagens, TGFβ1 targets, and integrin cell surface interactions. Similarly, signature genes involved in cell-cycle and downstream of IL6/JAK/STAT3 signaling and interferon α responses, among others, were preferentially downregulated by TGFβ. Finally, we selected a number of newly identified genes including CCN2,[35] TGFbi,[36] ADAM12,[36] BGN,[34] and genes that are associated with other types of fibrosis including LTBP2 and TPM1, all of which were validated in a replication cohort via quantitative polymerase chain reaction in the 781i mesenchymal cells (Supplementary Figure 1). This further confirms the applicability of our model to determining TGFβ responses.

Line-Specific Transcriptional Identity and Responses to TGFβ in iPSC-Derived Mesenchymal Cells

The previous multivariate analysis identified a common, global response to TGFβ in our panel of iPSC-derived mesenchymal cell lines. Gene set enrichment analysis performed on each iPSC line independently further confirmed that the magnitude and extent of this common response was similar across all lines (Figure 4A), and was not a consequence of data overfitting or a disproportionate response to TGFβ in one specific iPSC line. Therefore, we next aimed to evaluate if such a uniform behavior was the result of a lack of individual-specific signatures in our iPSC-derived HIOs or if line-specific gene expression could be observed. For each cell line, we again fitted our RNA-Seq data using a model that corrected for potential batch and technical effects and tested for line-specific gene expression using the pool of the remaining iPSC lines as a reference. For all 4 cell lines, we found at least 200 genes showing significant individual-specific expression levels (LRT-adjusted P value <.01). Although the focus of our study was determining the TGFb response in each line, we did observe differences in individual-specific baseline expression of various genes implicated in IBD such as several Rho and GTPase activity genes[37] in the 269i VEOIBD line (Figure 4B). To determine if our lines were suitable to assay individual-specific fibrotic responses, we fitted our RNA-Seq data to a model that included an interaction term between TGFβ treatment and individual gene expression to identify a set of 159 genes with a significant individual-specific response to TGFβ (LRT-adjusted P-value <.01). Further screening of these genes using an analysis performed on each iPSC line independently revealed that although in most cases the directionality of that response was similar across all iPSC lines (Figure 4C), the effect size was strikingly line specific, suggesting an enhanced response to TGFβ in some individuals and conserved in our mesenchymal HIOs. In summary, mesenchymal cells from iPSC-derived HIOs seem to conserve individual-specific baseline gene expression signatures and are potentially able to recapitulate personalized pro-fibrotic responses.

Fibrotic Responses and EMT Can Be Assayed in TGFβ-Treated iPSC-Derived Epithelial Cells

Previous reports have indicated that EMT may play a role in intestinal fibrosis,[15,16] and an organoid model utilizing murine biopsy-derived intestinal organoids has previously been used to model this in vitro.[38] Given that our mesenchymal model exhibited both generic and specific responses to TGFβ, we then wished to demonstrate as proof of principle that the epithelial component was also amenable to study. To achieve this, we generated epithelial eHIOs from one of our patient iPSC lines (CS781iCD-n3 iPSC) using a previously described protocol[39] and treated these with 2 different concentrations of TGFβ (0.5 ng/mL and 1 ng/mL) for 48 hours. We found a significant fold increase in a number of fibrosis-related genes including Col1a1, Col5a1, TIMP1, and FN after treatment with 1 ng/mL of TGFβ (Figure 5A). In addition, we also examined for changes in EMT-related genes including an epithelial marker, key transcription factors, and various mesenchymal markers. Interestingly, although changes in E-cadherin and Snai1 did not reach statistical significance and Twist2 was below the limit of detection, we did observe a significant increase in Twist1, Snai2, vimentin, and N-cadherin (Figure 5B). Finally, we examined untreated and treated eHIOs, and while there is little vimentin expression in untreated eHIOs, there is coexpression of both vimentin and E-cadherin in treated eHIOs (Figure 5C). This demonstrates that both the fibrotic response and EMT can be assayed in iPSC-derived epithelial cells.

Discussion

Intestinal fibrosis is a serious complication of CD, and research efforts are hampered by a lack of personalized in vitro cellular models. Here, we obtained iPSCs from 2 healthy control subjects and 2 VEOIBD patients with stricturing complications and subsequently generated HIOs from them. Although it has been widely alluded to, we first illustrated the variability of HIO culture by demonstrating the intra- and interline differences in the epithelial and mesenchymal populations of each organoid differentiation. Given this variability, we then developed a methodology that would allow purified populations of mesenchymal cells to be cultured (Figure 1D) so that responses to this specific cell type could be determined.

Numerous lines of evidence support that that the iPSC-derived approach may be useful to study the mechanisms of intestinal fibrosis. After carrying out a time course to assay the TGFβ response in the iPSC-derived mesenchymal cells, our finding of a 2- to 4-fold increase in N-cadherin is similar to what was previous reported,[32] and the increased Col1a1 expression in 3 of our 4 TGFβ-treated lines is also similar to previous reports using both the embryonic stem cell–derived model[19] and primary myofibroblasts.[40,41] Although we did not observe a change in the secretion of collagen, this could nonetheless be detected in the media and suggests that this model is amenable to testing for changes in the secretion of various extracellular matrix proteins. Our finding that numerous genes associated with intestinal fibrosis such as CCN2,[35] TGFbi,[36] ADAM12,[36] and BGN[34] were upregulated demonstrates the broad number of genes associated with intestinal fibrosis that could investigated using this model. Finally, the utility of this model was confirmed whereby, as expected,
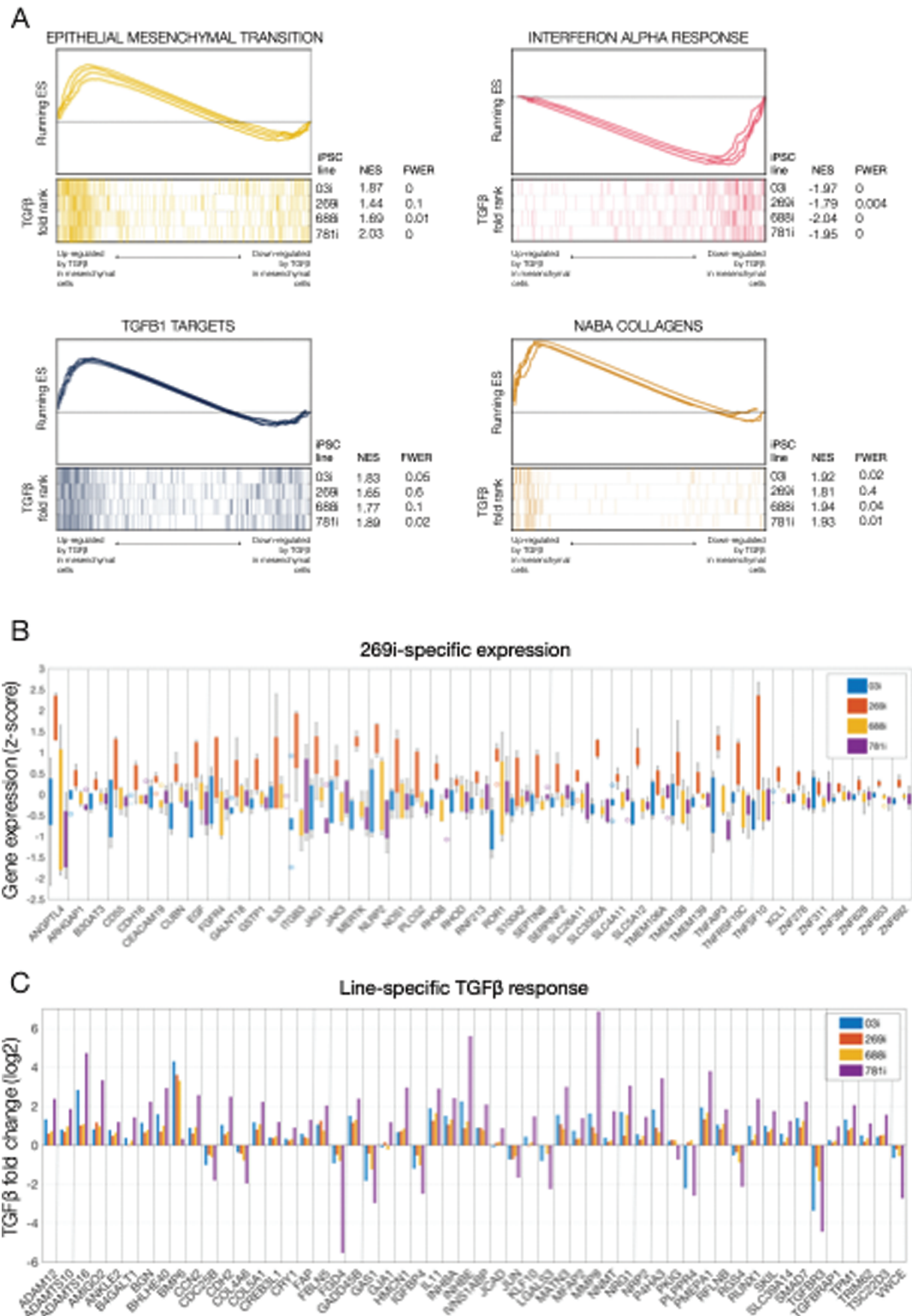
FIGURE 4. Line-specific transcriptional identity and responses to transforming growth factor β (TGFβ) in induced pluripotent stem cell (iPSC)–derived mesenchymal cells. A, Gene set enrichment analyses of selected enriched pathways in TGFβ-treated mesenchymal cells. The x-axis represents the preranked lists of genes based on the fold change between treated and untreated cells in each iPSC line independently. For each line, genes highly upregulated by TGFβ are positioned to the left. Segment plots (bottom) highlight the position of signature genes from independent reference pathways (eg, epithelial-mesenchymal transition) in each ranked list. The vertical axis in line plots (top) represents the cumulative enrichment score (ES) from gene set enrichment analysis of each signature set in each iPSC line. Normalized ES (NES) is the overall normalized ES (with familywise error rate [FWER]) for each selected pathway and iPSC line. B, Gene-wise boxplots of expression z-score distributions for selected genes showing line-specific expression in the 269i very early onset inflammatory bowel disease line. Each box represents a gene's z-score distribution for all samples in 1 experimental group (3
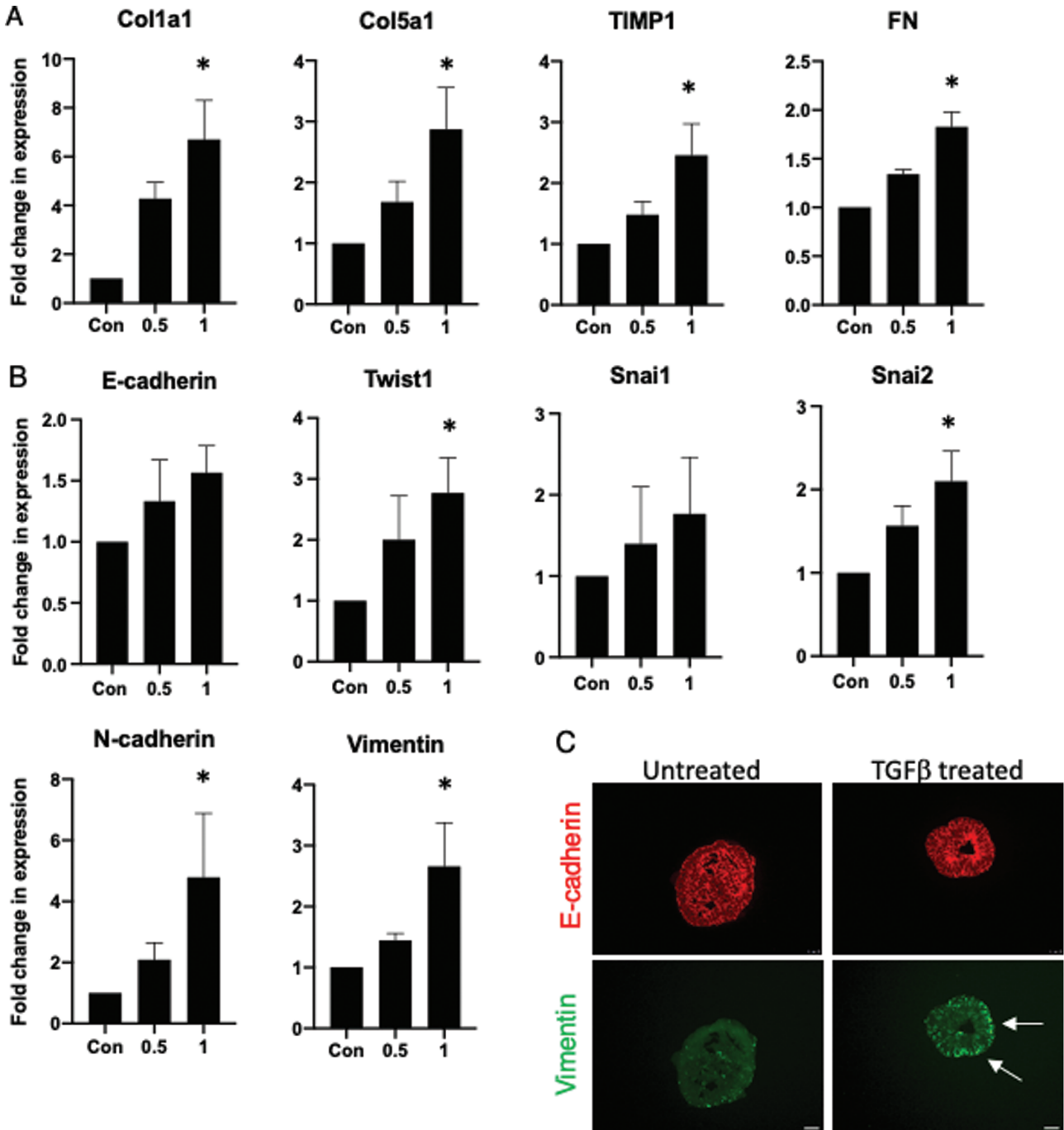
FIGURE 5. Characterization of fibrotic and epithelial-mesenchymal transition in transforming growth factor β (TGFβ)–treated induced pluripotent stem cell–derived epithelial cells. Fold change increases in (A) Col1a1, Col5a1, FN, and TIMP1 and (B) E-cadherin, Twist1, Snai1, Snai2, N-cadherin, and vimentin. Cells were assessed after 48 hours of 0 ng/mL, 0.5 ng/mL, and 1 ng/mL of TGFβ treatment. Data obtained from 3 independent experiments. C, Representative images showing epithelial-only human intestinal organoids after 48 hours of TGFβ (1 ng/mL) treatment and are immunopositive for E-cadherin (red) and vimentin (green). Scale bar = 25 μm. The white arrow points to coexpression of E-cadherin and vimentin. A Kruskal-Wallis test was carried out to determine for statistical significance at the different concentrations of TGFβ as compared with each respective untreated control subject. *$P < .05$.

the TGFβ signaling pathway was upregulated in response to TGFβ treatment and similar to our study examining the effect of interferon γ in iPSC-derived HIOs.[42]

Our hypothesis was that there would be a significant increase in fibrosis-related genes in mesenchymal cells derived from both VEOIBD patients as compared with the control lines, yet this was not observed. This may be explained by the fact that this was a study to establish the feasibility of this approach and so we included iPSC-derived cells from only 4 individuals, which is most likely underpowered to detect a differential response between the 2 groups. To address this, we have already initiated a study with increased

numbers of individuals to identify potential differences between groups. It also may be explained by the fact that intestinal stricturing is a highly heterogeneous condition that results from a combination of inflammation, intestinal fibrosis, or smooth muscle hypertrophy[8] and that intestinal fibrosis may also be initiated by other cytokines and microbes.[17] To address this, future studies will incorporate additional cytokines and microbes associated with this process and will also generate iPSCs from patients who have strictures that have a primarily fibrotic phenotype. Although the overall responses were broadly similar, our approach is strongly supported by the fact that there were differences in the lines both intrinsically and in their responses to TGFβ. This demonstrates that there are intrinsic differences between cells derived from each iPSC line and suggests the personalized responses are retained and can be determined using this modeling system.

While the main focus of our study was on our mesenchymal approach, we also assessed the feasibility of using iPSC-derived epithelial cells in our model. We observed that a TGFβ-induced fibrotic and EMT response could be examined in our eHIOs, with the significant increase in our selected mesenchymal-associated genes (N-cadherin and vimentin) being in agreement with previous reports.[43] Surprisingly there were no significant changes in E-cadherin expression, although this is in agreement with a previous study that assessed the effect of TGFβ on Caco2 cells.[44] We observed a significant increase in Twist1 and Snai2, which are key transcription factors in EMT and have been shown to be increased in various models of EMT.[43] Similarly, the finding of coexpression of both vimentin and E-cadherin has also previously been reported.[15,16] The agreement between our observations and previous studies supports the use of patient-specific epithelial cells in a highly controlled milieu as an invaluable model to examine the role of EMT in intestinal fibrosis.

Limitations of the study are as previously mentioned the low of individuals within the study. There is also a need to determine if the responses to various stimuli in a patient's iPSC-derived cells would correspond to those in their respective primary cells. Despite these limitations, this study suggests a new avenue to study intestinal fibrosis. The use of iPSC technology would permit the generation of a near unlimited number of patient-specific cell types. As this was the first time we were generating this type of model, we used TGFβ, as it is the cytokine most associated with fibrosis,[21] but it certainly suggests that the role of any cytokine or microbe could be tested and may also be amenable to testing various antifibrotic therapies in a personalized manner. Finally, we have previously reported that lymphoblastoid cell lines can be reliably reprogrammed to form iPSCs.[45] Given that there are lymphoblastoid cell lines available in well-characterized worldwide repositories that are linked to patient clinical history and long-term genotype-phenotype data, this system would now permit the in vitro modeling of intestinal fibrosis from well-defined patients with this complication of CD.

Conclusions

Here, we confirmed the feasibility of a personalized intestinal fibrosis model using purified populations of epithelial and mesenchymal cells from HIOs derived from iPSCs. We demonstrated that line-specific responses to the profibrotic cytokine TGFβ can be measured and thus offers a new avenue of research whereby a near unlimited number of biologically relevant cells can be generated for the in vitro modeling of intestinal fibrosis.

Supplementary Data

Supplementary data is available at *Inflammatory Bowel Diseases* online.

Conflicts of Interest

Cedars-Sinai and S.R.T. have financial interests in Prometheus Biosciences, Inc, a company which has access to the data and specimens in Cedars-Sinai's MIRIAD Biobank and seeks to develop commercial products.

References

1. Cosnes J, Cattan S, Blain A, et al. Long-term evolution of disease behavior of Crohn's disease. *Inflamm Bowel Dis.* 2002;8:244-250.
2. Louis E, Collard A, Oger AF, et al. Behaviour of Crohn's disease according to the Vienna classification: changing pattern over the course of the disease. *Gut.* 2001;49:777-782.
3. Cosnes J, Nion-Larmurier I, Beaugerie L, et al. Impact of the increasing use of immunosuppressants in Crohn's disease on the need for intestinal surgery. *Gut.* 2005;54:237-241.

4. Cosnes J, Bourrier A, Nion-Larmurier I, et al. Factors affecting outcomes in Crohn's disease over 15 years. *Gut*. 2012;61:1140-1145.

5. Jeuring SF, van den Heuvel TR, Liu LY, et al. Improvements in the long-term outcome of crohn's disease over the past 2 decades and the relation to changes in medical management: results from the population-based IBDSL cohort. *Am J Gastroenterol*. 2017;112:325-336.

6. Kugathasan S, Denson LA, Walters TD, et al. Prediction of complicated disease course for children newly diagnosed with Crohn's disease: a multicentre inception cohort study. *Lancet*. 2017;389:1710-1718.

7. Jostins L, Ripke S, Weersma RK, et al.; International IBD Genetics Consortium (IIBDGC). Host-microbe interactions have shaped the genetic architecture of inflammatory bowel disease. *Nature*. 2012;491:119-124.

8. Bettenworth D, Bokemeyer A, Baker M, et al; Stenosis Therapy and Anti-Fibrotic Research (STAR) Consortium. Assessment of Crohn's disease-associated small bowel strictures and fibrosis on cross-sectional imaging: a systematic review. *Gut*. 2019;68:1115-1126.

9. Shi Y, Inoue H, Wu JC, Yamanaka S. Induced pluripotent stem cell technology: a decade of progress. *Nat Rev Drug Discov*. 2017;16:115-130.

10. Sato T, Stange DE, Ferrante M, et al. Long-term expansion of epithelial organoids from human colon, adenoma, adenocarcinoma, and Barrett's epithelium. *Gastroenterology*. 2011;141:1762-1772.

11. VanDussen KL, Marinshaw JM, Shaikh N, et al. Development of an enhanced human gastrointestinal epithelial culture system to facilitate patient-based assays. *Gut*. 2015;64:911-920.

12. Spence JR, Mayhew CN, Rankin SA, et al. Directed differentiation of human pluripotent stem cells into intestinal tissue in vitro. *Nature*. 2011;470:105-109.

13. Gleeson JP, Estrada HQ, Yamashita M, et al. Development of physiologically responsive human iPSC-derived intestinal epithelium to study barrier dysfunction in IBD. *Int J Mol Sci*. 2020;21:1438.

14. Workman MJ, Gleeson JP, Troisi EJ, et al. Enhanced utilization of induced pluripotent stem cell-derived human intestinal organoids using microengineered chips. *Cell Mol Gastroenterol Hepatol*. 2018;5:669-677.e2.

15. Flier SN, Tanjore H, Kokkotou EG, et al. Identification of epithelial to mesenchymal transition as a novel source of fibroblasts in intestinal fibrosis. *J Biol Chem*. 2010;285:20202-20212.

16. Scharl M, Huber N, Lang S, et al. Hallmarks of epithelial to mesenchymal transition are detectable in Crohn's disease associated intestinal fibrosis. *Clin Transl Med*. 2015;4:1.

17. Rieder F, Fiocchi C, Rogler G. Mechanisms, Management, and Treatment of Fibrosis in Patients With Inflammatory Bowel Diseases. *Gastroenterology*. 2017;152:340-350.e6.

18. Lawrance IC, Rogler G, Bamias G, et al. Cellular and molecular mediators of intestinal fibrosis. *J Crohns Colitis*. 2017;11:1491-1503.

19. Rodansky ES, Johnson LA, Huang S, et al. Intestinal organoids: a model of intestinal fibrosis for evaluating anti-fibrotic drugs. *Exp Mol Pathol*. 2015;98:346-351.

20. Steiner CA, Rodansky ES, Johnson LA, et al. AXL is a potential target for the treatment of intestinal fibrosis. *Inflamm Bowel Dis*. 2021;27:303-316.

21. Yun SM, Kim SH, Kim EH. The molecular mechanism of transforming growth factor-β signaling for intestinal fibrosis: a mini-review. *Front Pharmacol*. 2019;10:162.

22. Dobin A, Davis CA, Schlesinger F, et al. STAR: ultrafast universal RNA-seq aligner. *Bioinformatics*. 2013;29:15-21.

23. Casero D, Sandoval S, Seet CS, et al. Long non-coding RNA profiling of human lymphoid progenitor cells reveals transcriptional divergence of B cell and T cell lineages. *Nat Immunol*. 2015;16:1282-1291.

24. Hoffman GE, Schadt EE. variancePartition: interpreting drivers of variation in complex gene expression studies. *BMC Bioinformatics*. 2016;17:483.

25. Love MI, Huber W, Anders S. Moderated estimation of fold change and dispersion for RNA-seq data with DESeq2. *Genome Biol*. 2014;15:550.

26. Zhou Y, Zhou B, Pache L, et al. Metascape provides a biologist-oriented resource for the analysis of systems-level datasets. *Nat Commun*. 2019;10:1523.

27. Shannon P, Markiel A, Ozier O, et al. Cytoscape: a software environment for integrated models of biomolecular interaction networks. *Genome Res*. 2003;13:2498-2504.

28. Huang DW, Sherman BT, Tan Q, et al. The DAVID gene functional classification tool: a novel biological module-centric algorithm to functionally analyze large gene lists. *Genome Biol*. 2007;8:R183.

29. Subramanian A, Tamayo P, Mootha VK, et al. Gene set enrichment analysis: a knowledge-based approach for interpreting genome-wide expression profiles. *Proc Natl Acad Sci U S A*. 2005;102:15545-15550.

30. Liberzon A, Subramanian A, Pinchback R, et al. Molecular signatures database (MSigDB) 3.0. *Bioinformatics*. 2011;27:1739-1740.

31. Liberzon A, Birger C, Thorvaldsdóttir H, et al. The Molecular Signatures Database (MSigDB) hallmark gene set collection. *Cell Syst*. 2015;1:417-425.

32. Burke JP, Cunningham MF, Sweeney C, et al. N-cadherin is overexpressed in Crohn's stricture fibroblasts and promotes intestinal fibroblast migration. *Inflamm Bowel Dis*. 2011;17:1665-1673.

33. McKaig BC, McWilliams D, Watson SA, Mahida YR. Expression and regulation of tissue inhibitor of metalloproteinase-1 and matrix metalloproteinases by intestinal myofibroblasts in inflammatory bowel disease. *Am J Pathol*. 2003;162:1355-1360.

34. van Haaften WT, Blokzijl T, Hofker HS, et al. Intestinal stenosis in Crohn's disease shows a generalized upregulation of genes involved in collagen metabolism and recognition that could serve as novel anti-fibrotic drug targets. *Therap Adv Gastroenterol*. 2020;13:1756284820952578.

35. Beddy D, Mulsow J, Watson RW, et al. Expression and regulation of connective tissue growth factor by transforming growth factor beta and tumour necrosis factor alpha in fibroblasts isolated from strictures in patients with Crohn's disease. *Br J Surg*. 2006;93:1290-1296.

36. Haberman Y, Minar P, Karns R, et al. Mucosal inflammatory and wound healing gene programs reveal targets for stricturing behavior in pediatric Crohn's disease. *J Crohns Colitis*. 2020;15:273-286.

37. Pradhan R, Ngo PA, Martínez-Sánchez LD, et al. Rho GTPases as key molecular players within intestinal mucosa and GI diseases. *Cells*. 2021;10:66.

38. Hahn S, Nam MO, Noh JH, et al. Organoid-based epithelial to mesenchymal transition (OEMT) model: from an intestinal fibrosis perspective. *Sci Rep*. 2017;7:2435.

39. Gleeson JP, Brayden DJ, Ryan SM. Evaluation of PepT1 transport of food-derived antihypertensive peptides, Ile-Pro-Pro and Leu-Lys-Pro using in vitro, ex vivo and in vivo transport models. *Eur J Pharm Biopharm*. 2017;115:276-284.

40. Zhao S, Dejanovic D, Yao P, et al. Selective deletion of MyD88 signaling in α-SMA positive cells ameliorates experimental intestinal fibrosis via post-transcriptional regulation. *Mucosal Immunol*. 2020;13:665-678.

41. Filidou E, Valatas V, Drygiannakis I, et al. Cytokine receptor profiling in human colonic subepithelial myofibroblasts: a differential effect of Th polarization-associated cytokines in intestinal fibrosis. *Inflamm Bowel Dis*. 2018;24:2224-2241.

42. Workman MJ, Troisi E, Targan SR, et al. Modeling intestinal epithelial response to interferon-gamma in induced pluripo-

tent stem cell-derived human intestinal organoids. *Int J Mol Sci.* 2020;22:288.

43. Kalluri R, Weinberg RA. The basics of epithelial-mesenchymal transition. *J Clin Invest*. 2009;119:1420-1428.

44. Buckley ST, Medina C, Ehrhardt C. Differential susceptibility to epithelial-mesenchymal transition (EMT) of alveolar, bronchial and intestinal epithelial cells in vitro and the effect of angiotensin II receptor inhibition. *Cell Tissue Res*. 2010;342: 39-51.

45. Barrett R, Ornelas L, Yeager N, et al. Reliable generation of induced pluripotent stem cells from human lymphoblastoid cell lines. *Stem Cells Transl Med*. 2014;3:1429-1434.